Journal of Applied Polymer Science

Thermal Stability of Novolac Cured with Polyborosilazane

Zibin Guo,[1,2] Hao Li,[2] Weijian Han,[2] Tong Zhao[2]
[1]Graduate School of the Chinese Academy of Sciences, Shijingshan District, Beijing, People's Republic of China 100039
[2]Institute of Chemistry, the Chinese Academy of Sciences, Haidian District, Beijing, People's Republic of China 100190
Correspondence to: T. Zhao (E-mail: tzhao@iccas.ac.cn)

ABSTRACT: To improve the thermal stability of phenolic resins, silicon- and boron-containing phenolic resin (SBPR) was synthesized from novolac-type phenolic resin using polyborosilazane (PBSZ) as curing agent, which can react with novolac resin at room temperature. The curing mechanism was studied by Fourier Transform infrared spectroscopy. The thermal and morphological properties of SBPR were studied by thermogravimetric analysis (TG) and scanning electron microscopy (SEM) respectively. TG results showed that the thermal properties of SBPR were much better than the corresponding novolac resin cured with hexamethylenetetramine, both for the initial decomposition temperatures (T_d) and residual weight at 900°C. The SEM and EDX results showed that the SBPR hybrids after oxidation were covered with SiO_2 glass coatings, which improved the thermo-oxidative resistance of SBPR. © 2012 Wiley Periodicals, Inc. J. Appl. Polym. Sci. 000: 000–000, 2012

KEYWORDS: curing of polymers; crosslinking; stabilization

Received 22 February 2012; accepted 6 August 2012; published online
DOI: 10.1002/app.38441

INTRODUCTION

Phenolic resin (PR) is one of the most common synthetic thermosetting resins. It has been widely used in the industry, such as adhesive, coating, laminates, and composites. Especially, because phenolic resin has good properties of heat resistance and heat ablation,[1] it was used as an irreplaceable ablative material in military and aerospace industries in applications such as space vehicles, rockets, missiles, etc.[2,3] The rapid development of PR applications has attracted many researchers to improve its thermal properties. To modify the thermal properties, silicon-containing compounds have been used and the effects have been discussed.[4–6] Boron-containing compounds have been also extensively introduced into phenolic resins by many researchers[2,7,8] exhibiting outstanding performance of flame retardancy and thermo-oxidative resistance, which was attributed to the formation of nonpenetrable glass coatings during thermal degradation.[8]

Novolac resin is a type of phenolic resin where the molar ratio of formaldehyde to phenol of less than one, and the phenol units are mainly linked by methylene groups. Hexamethylenetetramine (HMTA) is often used as curing agent to crosslink novolac by forming methylene and dimethylene amino bridges. Generally, the curing reaction with HTMA requires a relatively high temperature. In this work, silicon- and boron-containing phenolic resin (SBPR) was synthesized from novolac-type phenolic resin using polyborosilazane as curing agent, instead of HMTA. According to our research, novolac resin can be crosslinked by polyborosilazane at room temperature. The curing mechanism of SBPR was studied by Fourier-transform infrared spectrometry (FTIR), and the thermal stability and thermo-oxidative resistance of SBPR were monitored by thermogravimetry analysis (TGA) and scanning electric microscopy (SEM).

EXPERIMENTAL PROCEDURE

Materials

Novolac resin was purchased from ShangDong Shengquan Chemical. HMTA was purchased from Tianjin Guangfu Fine Chemical Research Institute. Diethyl ether was purchased from Sinopharm Chemical Reagent. PBSZ was synthesized in our laboratory according to the literature[9] ($M_w = 7142$, $M_w/M_n = 3.66$).

Preparation of Silicon and Boron Modified Phenolic Resin

The preparation of SBPR involved mixing two solutions, solution A and B. Solution A was novolac resin dissolved in diethyl ether with 40 wt % concentration, while solution B was PBSZ dissolved in the same solvent with the same concentration. The mixing weight ratios of B/A were selected at 10/100, 20/100, 40/100, and 100/100, which were also the weight ratios of PBSZ/novolac. The SBPR was prepared as follows: the solution B was added quickly into solution A with vigorous stirring at about 0°C. After stirred for 10 min, the mixture was poured into an aluminum foil box to form a gel at room temperature. The wet gel was aged in a vacuum oven at room temperature for 24 h,

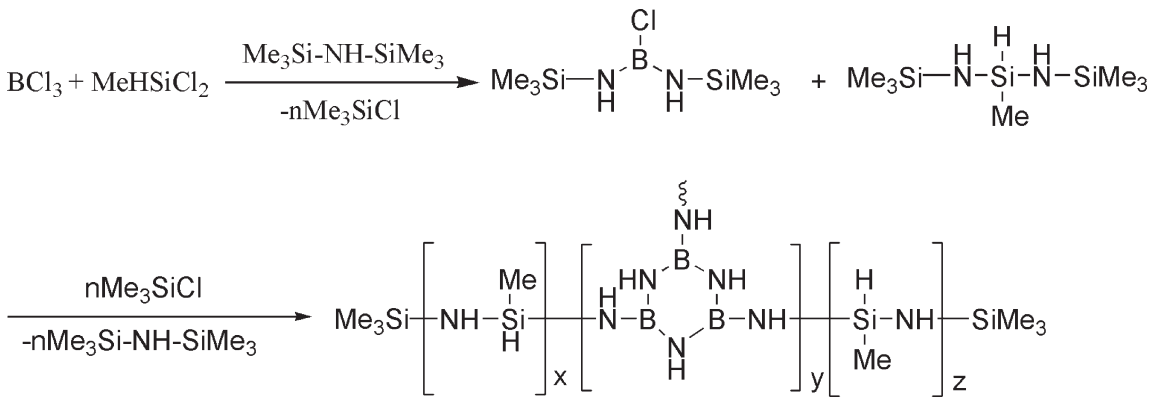

Scheme 1. The synthesis and chemical structure of PBSZ.

followed by post-curing process at different temperatures. The nomenclature of the samples is presented as *x*-PBSZ-*T*-*t*, where *x* is the mixing weight ratio of PBSZ/novolac, and *T* and *t* represent the postcuring temperature and time respectively. For example, 40%-PBSZ-120°C-6 h represents SBPR sample prepared with PBSZ/novolac weight ratio at 40% and postcured at 120°C for 6 h. If not mentioned, all SBPR samples were cured at 150°C for 4 h. Novolac resin cured with 10 wt % HTMA was also prepared as a comparison, and the curing condition was set at 180°C for 4 h.

Instrumentation

FTIR were recorded between 4000 and 400 cm^{-1} with a Bruker Tensor 27 IR spectrometer. ^{11}B-NMR spectra were performed in $CDCl_3$ solution with 0.1 wt % $Cr(acac)_3$ as relaxation agent on a Brucker DMX 300 instrument using tetramethylsilane (TMS) as an external standard. The gelling time test was carried out on a plate with depressions in the form of segments of spheres according to ISO 8987-2005, and the testing temperature was set at 0°C. Thermogravimetric analysis (TGA) was carried out on a Netzsch STA 409 PC instrument from room temperature to 900°C in N_2 or air atmosphere with ramping rate of 10°C/min. All samples were ground into fine powder, and then dried under vacuum at 30°C for 4 h before testing. The morphology of the SBPR samples was examined using a scanning electron microscope (SEM, S-4800), and the distribution of elements in the SBPR hybrids were obtained by SEM EDX mapping technology (SEM, S-4800). X-ray photoelectron spectroscopy (XPS) experiments were performed on a VG scientific ESCALab220i-XL photoelectron spectrometer equipped with a twin anode, providing unchromatized Al Kα radiations (1486.6 eV). The spectrometer, which was equipped with a multichannel detector, operated at 300 W and the C1s (284.8 eV) was chosen as the reference line.

RESULTS AND DISCUSSION

Characterization of Polyborosilazane

PBSZ was synthesized in our laboratory via a cocondensation approach using methyldichlorosilane ($MeHSiCl_2$), boron trichloride (BCl_3), and hexamethydisilazane (HMDZ) as starting materials according to the literature[9] as shown in Scheme 1. Instead of generally being used as a polymeric precursor to SiBNC ceramic, PBSZ was used as a new curing agent to crosslink novolac-type penolic resin in this work. The final structure of PBSZ was characterized by FTIR spectrum, as shown in Figure 1. The absorption peaks around 3380–3400 cm^{-1} and 2150 cm^{-1} can be attributed to N—H stretching vibration[10] and Si—H stretching vibration[11] respectively. The absorption peaks at 1386 cm^{-1} and 913 cm^{-1} can be attributed to B—N and Si—N stretching vibration[9] respectively. The existence of the B_3N_3 rings in PBSZ is proven by the characteristic N—B—N vibration bands[9] at 1450 cm^{-1}.

NMR spectra of the polymer were also measured to confirm the structure. As shown in Figure 2, the ^{11}B-NMR spectrum of PBSZ in $CDCl_3$ appears a single peak centered at 27.8 ppm, illustrating that only borazinic BN_3 environment exists in the polymer.[9] Figure 3 shows ^{29}Si-NMR spectrum of PBSZ. The resonances at 2.5 ppm and −21.74 ppm are assigned to Si atom in the —NH—$SiMe_3$ and —HN—Si(HMe)—NH— groups respectively.[10]

Curing Mechanism

To study the reaction mechanism of the phenolic group with PBSZ, phenol was used as the model compound. The PBSZ/phenol mixture was prepared as the same way as PBSZ/novolac mixture as described in the experimental part, and aged in a vacuum oven at room temperature for 24 h. Figure 4 shows the

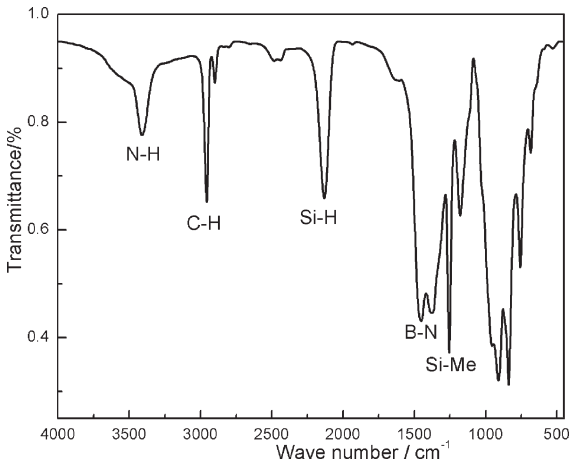

Figure 1. Infrared spectrum of PBSZ.

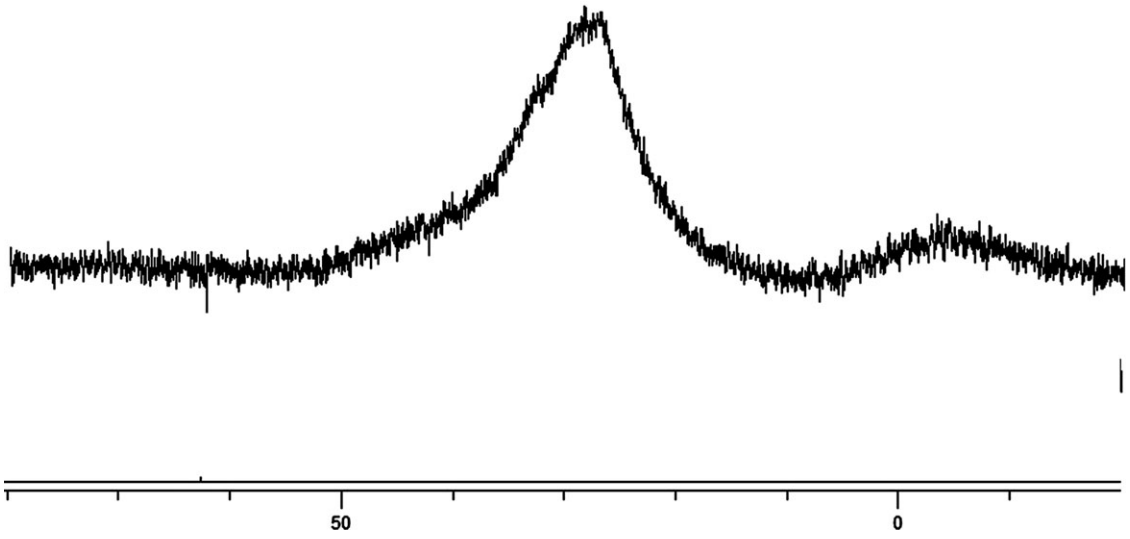

Figure 2. ^{11}B-NMR spectrum of PBSZ.

infrared spectrum of the reaction mixture in which the weight ratio of PBSZ/phenol was 40/100. In this reaction, the phenolic hydrogen was nearly completely replaced, which was evidenced by the disappearance of the absorption of phenolic O—H in-plane deformation at 1236 cm^{-1}. The decrease of absorption of Si—N stretching at 839 cm^{-1} and N—H deformation at 1178 cm^{-1}, and the appearance of the new absorption of C—O—Si and O—Si—O stretching in the 1000–1100 cm^{-1} region, showed that the Si—N bond ruptured in the reaction, Si—O bond formed, and NH_3 was excluded. Meanwhile, B—O bond formed and B—N bond ruptured, implied by the disappearance of B—N stretching at 1448 cm^{-1} and the appearance of B—O stretching at 1403 cm^{-1}. On the basis of the results of FTIR analysis, the reaction mechanism of phenol with PBSZ was inferred as shown in Scheme 2.

NMR spectra of the PBSZ/phenol mixture were also measured to confirm the structure. Figure 5 shows ^{11}B-NMR spectrum of the PBSZ/phenol mixture. The resonances at 1.92 and 14.10 ppm can be attributed to B atom in the BO_3 structure and partially reacted srructure BNO_2 respectively. Figure 6 shows ^{29}Si-NMR spectrum of the mixture. The resonance at −20.86 ppm is assigned to Si atom in the -HN-Si(HMe)-NH- group of the PBSZ.[10] Meanwhile, there are two new resonances at −27.74 ppm and −38.27 ppm can be atributed to Si atom in the —O—Si(HMe)—NH— and —O—Si(HMe)—O— respectively.

As the Si—N and B—N bonds can react with phenolic O—H bond, PBSZ was used as a new curing agent to crosslink novolac resin in this work. Four different ratios of PBSZ/novolac mixture were prepared with the standard procedure as described in the experimental part, and the gelling time was summarized in Table I. Figure 7 shows the infrared spectrum of SBPR resins with different ratios of PBSZ/novolac cured at 30°C for 24 h. The benzene ring absorption at 1598 cm^{-1} was used as the internal standard. As the weight ratios increased, the absorption of phenolic O—H in-plane deformation at 1236 cm^{-1} decreased, while the absorption of Si—N stretching at 839 cm^{-1} and B—N stretching at 1448 cm^{-1} increased. In the spectrum of 10%-PBSZ sample, the phenolic O—H bond was excessive showing the curing of novolac was not complete. In the spectrum of 100%-PBSZ sample, the novolac was insufficient, implied by the disappearance of absorption of phenolic O—H bond and the remain of the absorption of Si—N and B—N

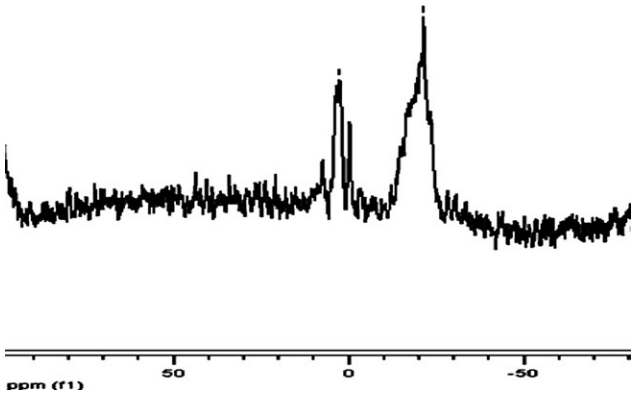

Figure 3. ^{29}Si-NMR spectrum of PBSZ.

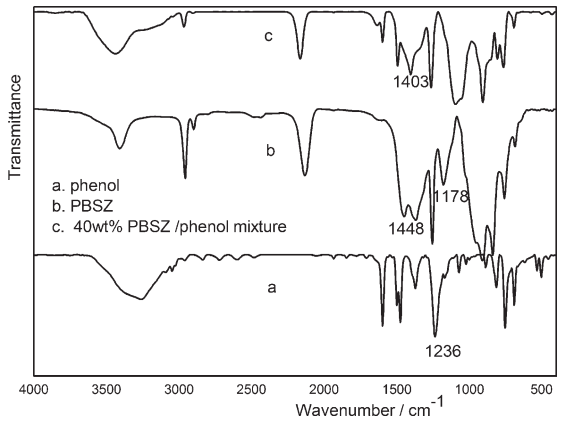

Figure 4. Infrared spectrum of phenol and PBSZ mixture.

Applied Polymer SCIENCE

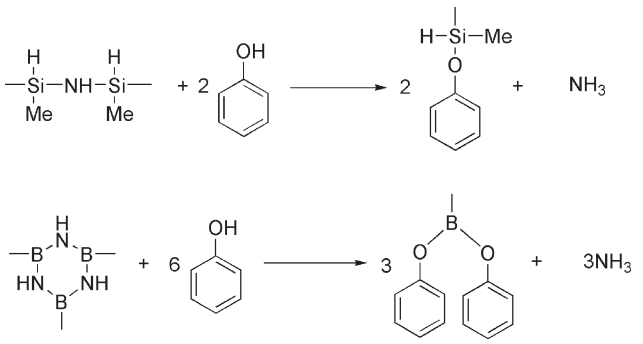

Scheme 2. The reaction mechanism of phenol with PBSZ.

bond. In the spectrum of 20%-PBSZ and 40%-PBSZ samples, the absorption of phenolic O—H bond, Si—N, and B—N bond both remained, the reactions were not complete. It could be attributed to short gelling time of the reaction mixture because of the high reactivity of PBSZ with novolac resin.

Distribution and Content of Si and B Element

Figure 8 illustrates the distribution of Si and B elements in the 40%-PBSZ sample obtained by SEM EDX mapping technology. The white points in the figures denote the Si or B atoms. The result demonstrates that the distribution of inorganic elements inside SBPR hybrid is homogeneous.

XPS analysis was used to further reveal the curing mechanism. The main component contents of the PBSZ and 40%-PBSZ-30°C-24h were detected, and the data were summarized in Table II. It can be found that the ratio of N/Si in the SBPR hybrid sample is much lower than that in the PBSZ, confirming that the N converted into NH_3 and excluded in the curing process. Meanwhile, there was still a little nitrogen remain in the SBPR hybrid, which indicates the uncompleted curing process.

Thermal Stability

TG analysis was carried out under nitrogen and air to determine the thermal stability of the SBPR resins. To study the effect of temperature on the thermal properties, Figure 9 shows the TG and DTG patterns of the 40%-PBSZ hybrids cured at different temperatures, and Table III gives TGA data for the weight loss with temperature. As the curing temperature increases, the thermal stability of 40%-PBSZ increases slowly at first and dramatically subsequently, both for the initial decomposition temperature and char yields. From the DTG curves, it can be seen that the first decomposition peak move to higher temperature with the increase of curing temperature. When the curing temperature increased up to 150°C, the first decomposition peak disappeared completely. It can be attributed to the complete removal of the solvent and the byproduct during the curing process. As mentioned before, in spite of the high reactivity between novolac resin and PBSZ, the curing process was not complete at relatively low temperature because of the solid state of the two compounds. When the curing temperature increased up to 150°C, the novolac resin became fluid and promoted the complete curing process.

The DTG patterns show that all 40%-PBSZ resins cured at different temperatures shared the same main decomposition peak, which centered at about 590°C. It can be inferred that the effect of curing temperature on the thermal stability of SBPR resins was mainly limited in the low temperature area (below 200°C).

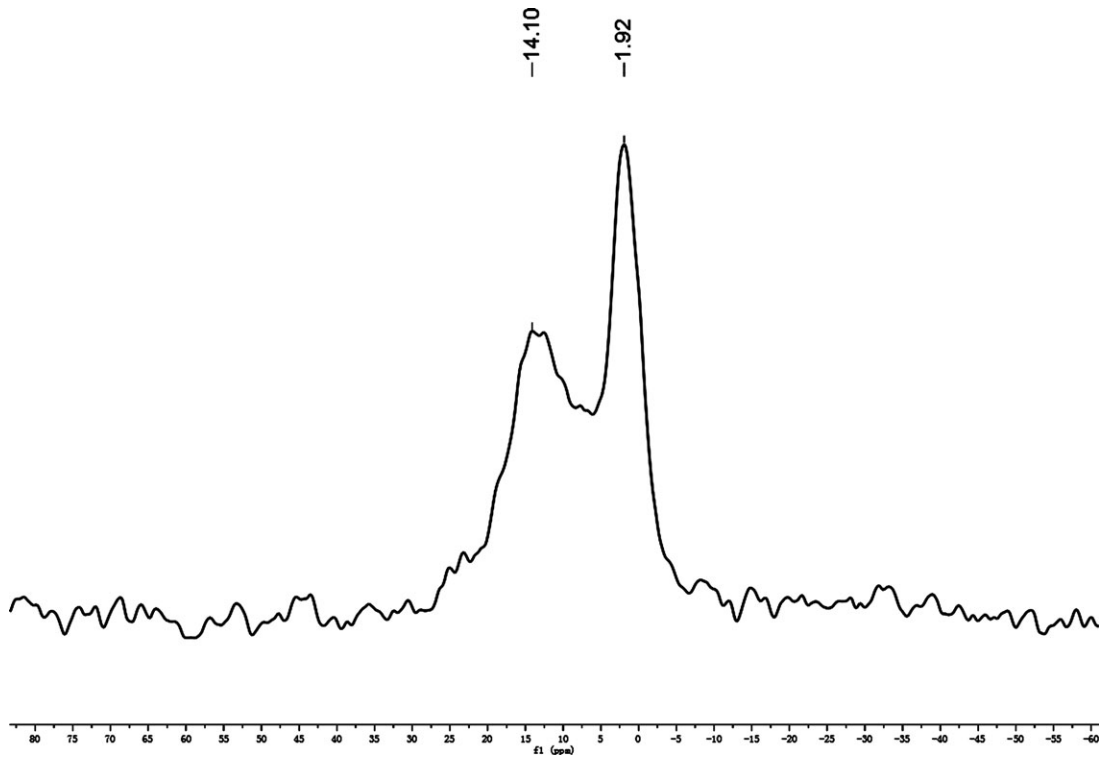

Figure 5. ^{11}B-NMR spectrum of phenol and PBSZ mixture

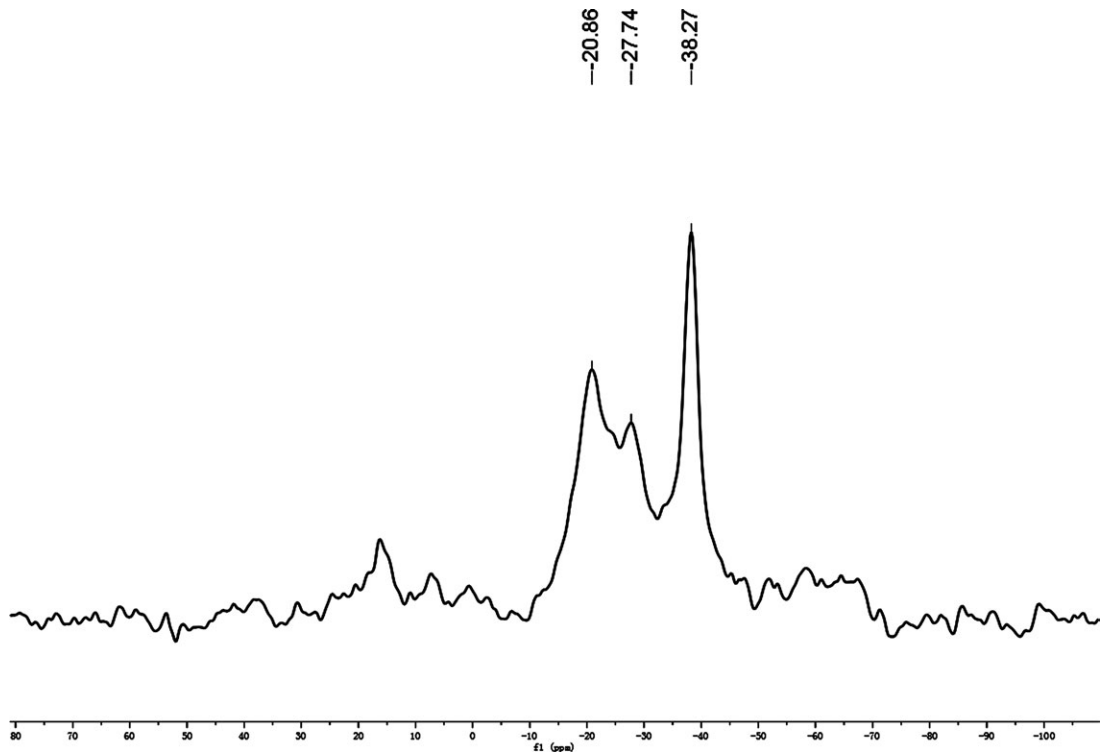

Figure 6. ^{29}Si-NMR spectrum of phenol and PBSZ mixture.

Actually, SBPR resins cured at low temperature experienced further curing process in the initial stage of the TGA experiment and caused weight loss due to the release of residual solvent and byproduct. As the novolac resin can be cured with PBSZ and its analogue at room temperature, it can be inferred the potential application of this reaction in chemical surface treatment.

Figure 10 shows TG plots of the SBPR samples prepared with different PBSZ/novolac mixing ratios and pure novolac resin cured with 10 wt % HTMA, and Table IV gives TGA data for the weight loss with temperature. Under N_2 atmosphere, as the weight ratios of PBSZ/novolac increased, the initial decomposition temperature of the SBPR increased first, and then deceased subsequently. The 40%-PBSZ sample shows dramatic improvement of thermal stability compared to unmodified novolac resin, the temperature of 5% loss weight increased 139°C. The char yield of 40%-PBSZ was 14.83% percent more than that of the unmodified resin.

Under air atmosphere, the initial decomposition temperature of the SBPR resins shared the same trend as under N_2 atmosphere, which increased at first and then deceased subsequently with the increase of PBSZ/novolac mixing ratios. The 40%-PBSZ sample shows dramatic improvement of oxidative resistance compared to unmodified novolac resin. The temperature of 5% loss weight of 40%-PBSZ sample increased 207°C. Compared to char yields obtained under N_2 atmosphere, significant differences of that under air between modified and unmodified phenolic resins were observed. While the char yield of unmodified novolac resin is practically nonexistent, the SBPR resins remained char yields approximately linear to the PBSZ content. Thus the PBSZ played decisive role in the char formation under air. Because char yield has been correlated to flame retardancy, these SBPR resins were expected to have good flame retardant properties.[7]

Table I. The Gelling Time of SBPR Samples Obtained at 0°C

Samples	Gelling time
10% PBSZ	>24 h
20% PBSZ	≈ 40 min
40% PBSZ	≈ 10 min
100% PBSZ	<1 min

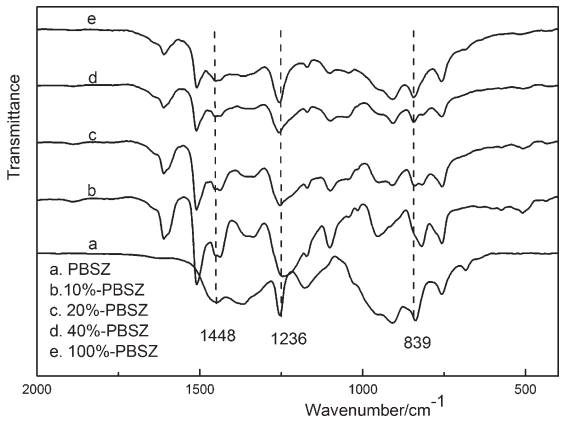

Figure 7. Infrared spectrum of SBPR resins.

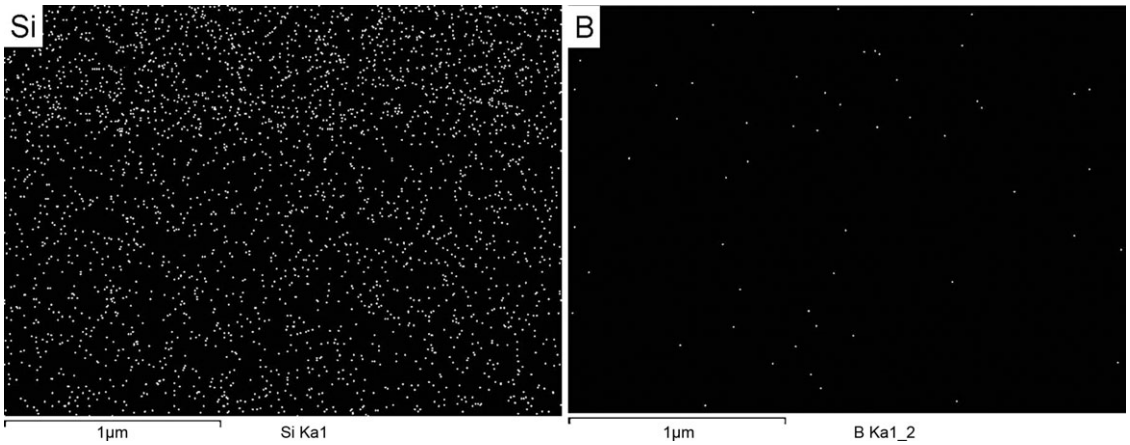

Figure 8. Distribution of inorganic elements in 40 wt % SBPR sample obtained by SEM EDX mapping technology.

Figure 11 shows that DTG patterns of the neat phenolic resin and 40%-PBSZ sample performed in nitrogen and air atmosphere. Under N_2 atmosphere, according to these curves, the degradation process experienced three decomposition peaks for the neat resin and two peaks for the modified. In the initial stage, the first peak for the neat and modified resins are both at about 220°C, which may correspond to the loss of some small end groups. Differences were observed in the following stage, that the neat resin appears the second decomposition peak at about 400°C, while the modified resin keeps steadily. The decomposition peak for the neat pehonlic resin at 400°C can be attributed to the depolymerization of the main chains with release of phenol and larger species of its derivatives.[7] As the modified phenolic resin was cross-linked by the PBSZ as well as the methylene bond, the disruption of the latter does not necessarily make the hybrid yield phenol or its derivatives. The third decomposition peak at 551°C for the neat resin and the second peak at 591°C for the modified resin may correspond to the rupture of phenolic O—H bond and charring of the resins, with release of benzene and its derivatives.[12] As the Si—O—C or B—O—C bond is firmer than the H—O—C bond, the decomposition peak of the modified resin is 40°C higher than that of the neat resin.

Under air atmosphere, the degradation process experienced similar stage between the neat and the modified resins. The DTG patterns of both neat and modified resins in air appeared almost as the same patterns as in N_2 environment before 400°C, indicating that the influence of the atmosphere on the degradation is nonsignificant in the low temperature area. At higher temperature, the DTG curves of both the neat and modified resins, turned from the typical single bell-shaped DTG patterns obtained in the nitrogen environment into a two-peak curves in

Table II. XPS Data of the Pure PBSZ and 40%-PBSZ-30°C-24 h Hybrid

	PBSZ		40%-PBSZ-30°C-24 h	
Element	Area	Atom concentration ratio (%)	Area	Atom concentration ratio (%)
C1s	57,348.95	50.47	52,995.9	57.19
O1s	31,549.97	10.88	58,874.72	24.91
N1s	29,555.88	15.33	2309.48	1.47
Si2p	17,950.83	17.76	12,035.32	14.61
B1s	3215.52	5.56	859.41	3.83

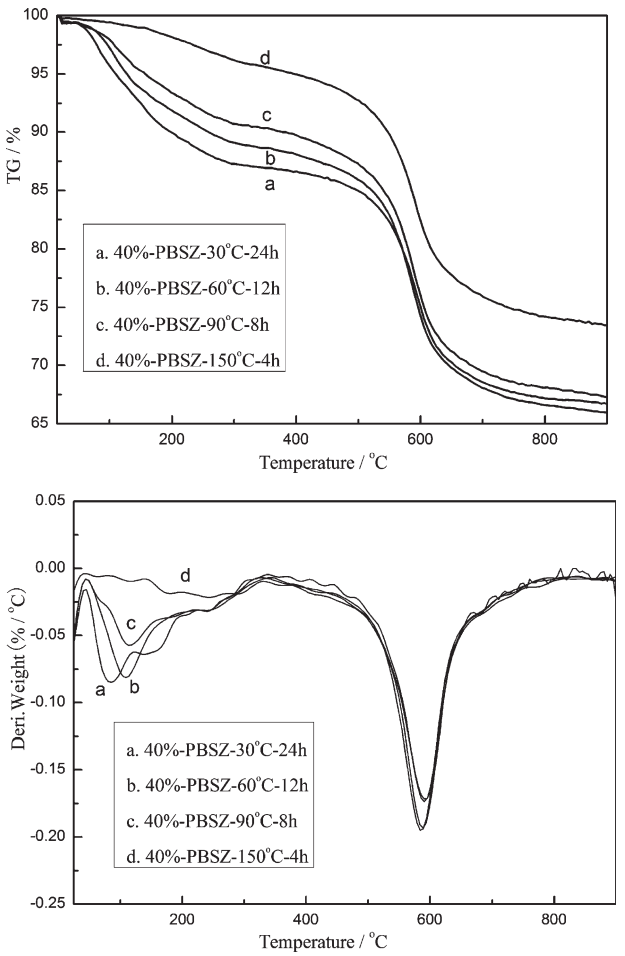

Figure 9. TG and DTG plots of 40% SBPR resins cured at different temperature (N_2, 10°C/min).

Table III. TGA Data of 40%-PBSZ Resins Postcured at Different Temperature

	TGA, N_2		
Samples	$T_{5\%}$ (°C)	T_{peak} (°C)	Residue at 900°C (%)
40%-PBSZ-30°C-24 h	109.6	592.0	66.65
40%-PBSZ-60°C-12 h	127.9	586.5	65.91
40%-PBSZ-90°C-8 h	156.9	589.0	67.26
40%-PBSZ-150°C-4 h	398.0	591.0	73.40

the presence of the oxidative atmosphere. Besides the first main peak centered at 568°C for the neat resin and 578°C for modified resin, another peak with comparable intensity centered at 646°C and 688°C appeared, respectively. This secondary main peak related to the combustion process due to the interaction of the matrix with oxygen.[5] This indicates that the degradation of the SBPR resins is a thermal-oxidative reaction in air, comparing to be a thermal decomposition process in nitrogen.

SEM and EDS Characterization of Oxidized Hybrid Materials

To study the thermo-oxidative resistance of the SBPR hybrid, 40%-PBSZ sample was calcined at 700°C for 30 min under air.

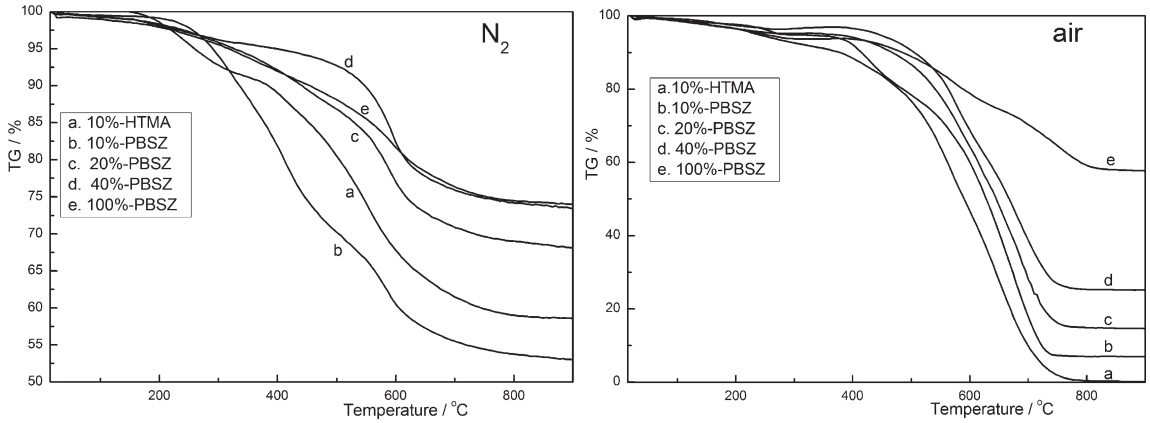

Figure 10. TG plots of SBPR resins cured with different contents of PBSZ and pure novolac resin cured with 10 wt % HTMA (10°C/min, N_2, air).

Table IV. TGA Data of SBPR and Pure Phenolic Resins

	TGA, N_2			TGA, air		
Samples	T_d^5 (°C)	T_{peak} (°C)	Residue (900°C, %)	T_d^5 (°C)	T_{peak} (°C)	Residue (900°C, %)
10% HTMA	259.7	401.2/551.6	58.57	235.8	568.0/646.5	0.14
10% PBSZ	290.2	411.2/581.7	52.97	274.2	427.3/667.9	6.86
20% PBSZ	326.9	589.0	68.04	360.5	584.7/680.0	14.60
40% PBSZ	398.0	591.0	73.40	442.9	577.6/688.2	25.10
100% PBSZ	316.8	591.6	73.98	248.0	573.0/759.5	57.67

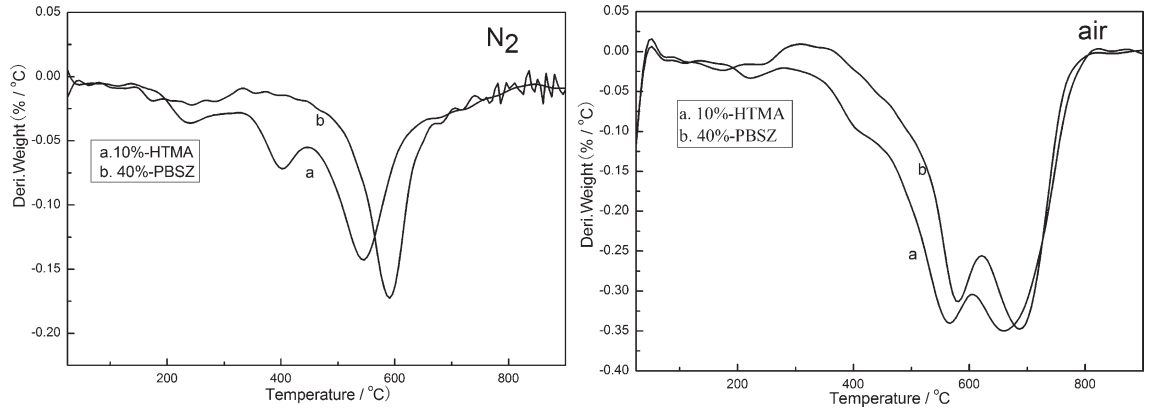

Figure 11. DTG plots of SBPR cured with 40 wt % PBSZ and pure novolac resin cured with 10 wt % HTMA (10°C/min, N_2, air).

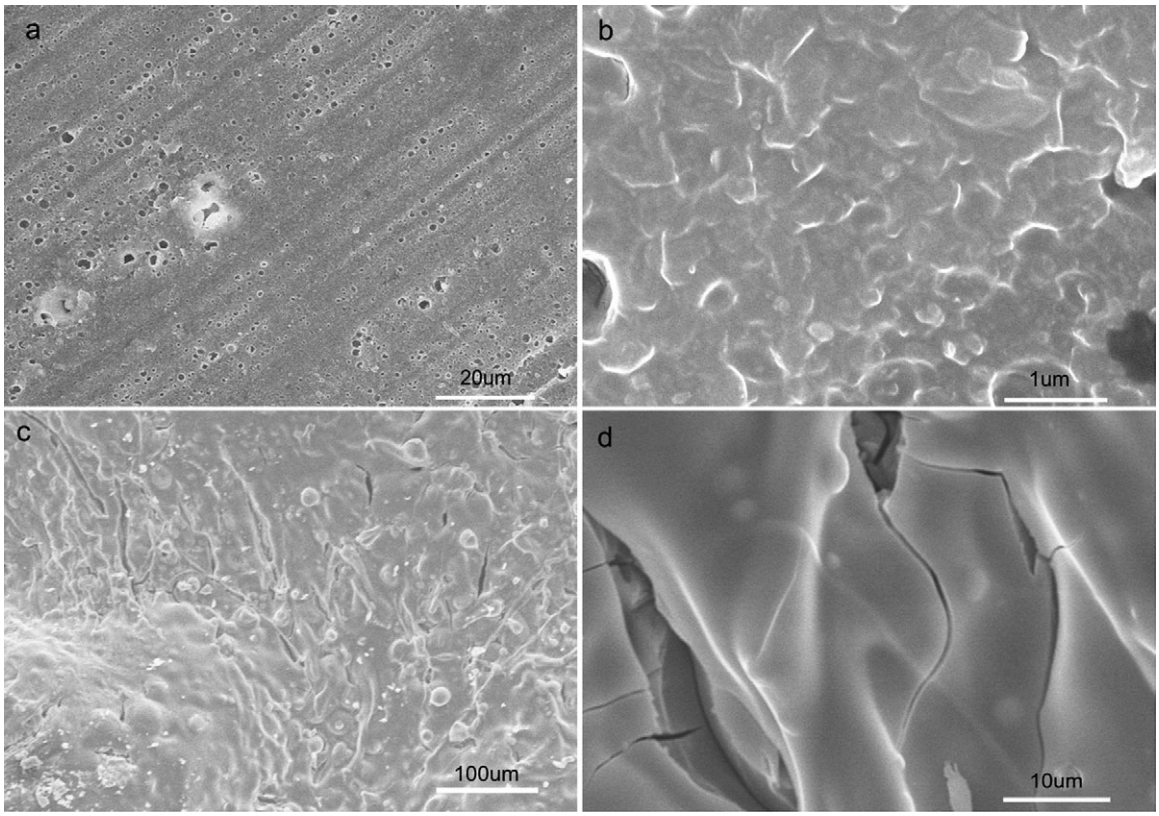

Figure 12. SEM photographs of 40% SBPR: (a, b) before oxidation; (c, d) after oxidation.

Figure 12 presents the morphological properties of SBPR hybrid before and after calcination. As shown in Figure 12(a,b), the surface of the SBPR sample was not smooth and continuous, which could be attributed to the release of the solvent and low-molecule by-product such as NH_3 in the curing process. Figure 12(c,d) represent the morphology appearance of the SBPR hybrid after oxidation at 700°C. The SiO_2 coatings, which have been confirmed by EDX analysis (Figure 13), distribute uniformly on the surface of the oxidized samples except for some crack. The better oxidation resistance of the PBSZ cured phenolic resin could be attributed to the protective SiO_2 coatings, which isolated the inner part of the hybrid sample from the oxidized atmosphere. However, boron atoms were not found on the surface of the oxidized hybrid samples, which can be attributed to detection limit of the instrument.

CONCLUSIONS

SBPR was synthesized from novolac-type phenolic resin using polyborosilazane (PBSZ) as curing agent, which can react with phenolic resin at room temperature. The thermal stability of SBPR was much better than the corresponding novolac resin cured with hexamethylenetetramine (HMTA), both for the initial decomposition temperatures (T_d) and residual weight. The

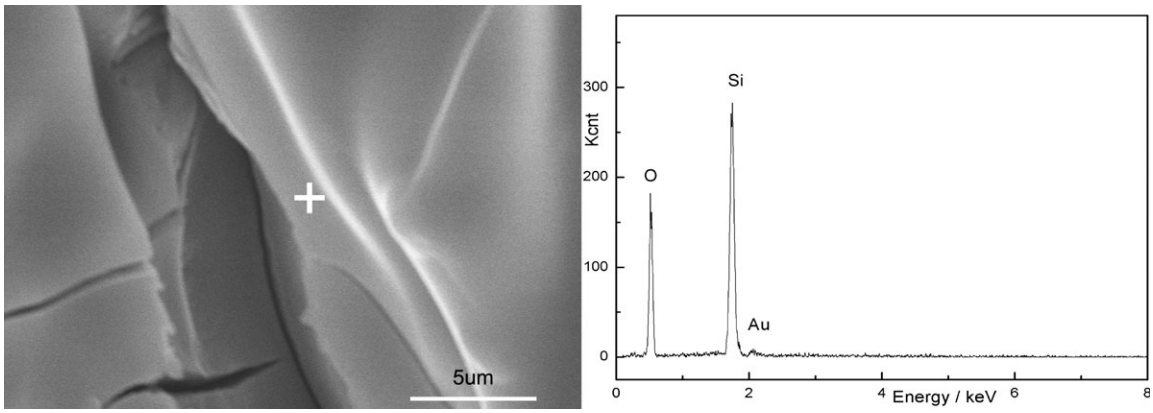

Figure 13. The EDS spectrum of the 40% SBPR sample after oxidation.

degradation process of SBPR experienced two decomposition peaks, differing from three peaks of the neat resin under N_2 atmosphere, while the degradation process of the modified resins shared two-peak curves with the neat resins in the presence of the oxidative atmosphere, indicating that the degradation of the modified phenolic resins is a thermal-oxidative reaction in air, comparing to be a thermal decomposition process in nitrogen. The better thermo-oxidative resistance of the SBPR resins could be attributed to the formation of the nonpenetrable glass coatings of SiO_2 in the thermal-oxidative process, which prevented further oxidation of the phenolic hybrids.

REFERENCES

1. Bahramian, A. R.; Kokabi, M.; Navid-Famili, M. H.; Beheshty, M. H. *Polymer* **2006,** *47*, 3661.
2. Abdalla, M. O.; Ludwick, A.; Mitchell, T. *Polymer* **2003,** *44*, 7353.
3. Higgins, A. *Int. J. Adhes. Adhes.* **2000,** *20*, 367.
4. Chen-Chi, M. M.; Jia-Min, L.; Wen-Chi, C.; Tse-Hao, K. *Carbon* **2002,** *40*, 977.
5. Natali, M.; Monti, M.; Kenny, J.; Torre, L. *J. Appl. Polym. Sci.* **2011,** *120*, 2632.
6. Zucheng, F.; Jinping, S. *J. Appl. Polym. Sci.* **2011,** *119*, 744.
7. Martin, C.; Ronda, J. C.; Cadiz, V. *Polym. Degrad. Stab.* **2006,** *91*, 747.
8. Duan-Chih, W.; Geng-Wen, C.; Yun, C. *Polym. Degrad. Stab.* **2008,** *93*, 125.
9. Yun, T.; Jun, W.; Xiaodong, L.; Wenhua, L.; Hao, W. *J. Inorg. Mater.* **2008,** *23*, 525.
10. Antler, M.; Laubengayer, A. W. *J. Am. Chem. Soc.* **1955,** *77*, 5250.
11. Weinmann, M.; Kamphowe, T. W.; Schuhmacher, J.; Muller, K.; Aldinger, F. *Chem. Mater.* **2000,** *12*, 2112.
12. Yanfang, L.; Jungang, G.; Rongzhen, Z. *Polym. Degrad. Stab.* **2002,** *77*, 495.